encit 2020

ABCM Associação Brasileira de Engenharia e Ciências Mecânicas

18th Brazilian Congress of Thermal Sciences and Engineering
November 16–20, 2020 (Online)

ENC-2020-0265
PREDICTION OF THE HEAT TRANSFER COEFFICIENT DURING CONDENSATION OF HYDROCARBONS IN MINI/CONVENTIONAL CHANNELS USING MACHINE LEARNING ALGORITHMS

Gabriel Furlan
Ghehardt Ribatski
Heat Transfer Research Group – HTRG, Department of Mechanical Engineering, São Carlos School of Engineering (EESC), University of Sao Paulo (USP), Av. Trabalhador São-Carlense, 400, Parque Arnold Schimidt, CEP: 13566-590, São Carlos, Brazil.
gabriel.furlan.sf@gmail.com
ribatski@sc.usp.br

Abstract. *This study investigates the use of machine learning (ML) method for predicting the heat transfer coefficient (HTC) during condensation of hydrocarbons in mini/conventional channels. The multi-layer perceptron with backpropagation (MLPB) and the gradient boosted decision tree (GBDT) algorithms are optimized, trained and validated based on experimental data gathered from the literature, which include results for propane, propylene, isobutene and ethane, tube diameters from 0.956 to 20.8 mm, mass velocities from 35 to 1000 kg/m²s and reduced pressures from 0.1 to 0.96. In order to capture the main mechanisms acting on the condensation process, dimensionless numbers Bond, Galileo, Reynolds and Weber were used as input parameters. The gradient boosted decision trees provided the best predictions with a mean absolute error (MAE) of 4.7% and 86.5% of the data predicted within an error band of ±10%. The neural net predicted 91.2% of the results within an error band of ±20% and a MAE of 8.5%. The ML methods successfully predict the effects on the HTC of vapor quality, mass velocity, saturation temperature, channel diameter and flow pattern. When applied to non-hydrocarbon data, the MLPB provided better predictions than GBDT, which may indicate that the first captures the experimental trends of the HTC. Moreover, based on a simulation of a tube-in-tube condenser, it was found that the ML methods need 90% lower processing time than Cavallini et al. (2006) model.*

Keywords: *condensation, hydrocarbon, heat transfer, machine learning*

1. INTRODUCTION

In the condenser design, an accurate prediction of the heat transfer coefficient is needed once it is related to the size of the heat exchanger and, therefore, to the amount of refrigerant contained inside it. The HTC is strictly linked to the two-phase flow topology, which depends on several factors, such as fluid properties (density, viscosity), operating conditions (pressure and temperature) and flow parameters (mass velocity, channel diameter, geometry and orientation, vapor quality). To overcome the difficulties in characterizing the condensation process, a promising option for predictive methods for condensation heat transfer is applying machine learning technics, which algorithms can learn nonlinear relations between inputs and outputs in an efficient way.

The artificial neural networks (ANN) have been widely applied for regression problems in distinct areas. Mohanraj et al. (2015) presented a state-of-the-art review of studies concerning the application of artificial neural networks for thermal analysis of heat exchangers and they highlighted remarkable results obtained from using ANN methodologies. Despite the sharp growth of works in the last two decades, most of the studies considered modeling the heat exchangers and not estimating the design parameters. The authors found only two works about condensation heat transfer (Demir et al., 2009; Balcilar et al., 2011), and none of them includes minichannel condensation. The two aforementioned works and two more recent studies performed by Azizi and Ahmadloo (2016) and López-Belchí et al. (2018) obtained excellent results using ANN to predict the condensation HTC. However, in these studies the ANN was applied for a reduced range of experimental conditions. López-Belchí et al. (2018) were the only ones to consider minichannel condensation, and also a broader range of experimental conditions. Nevertheless, the authors obtained reasonable results concerning HTC predictions.

The gradient boosted decision tree, a machine learning method recently proposed and yet not used in two-phase flow studies as far the present authors know, have outperformed ANN in several heat transfer analysis available in literature, e.g.: energy consumption in buildings (Touzani et al.,2018; Gong et al., 2020); solar thermal energy systems (Ahmad et al., 2018); heat transfer of oscillating heat pipes (Qian et al, 2020). Besides the greater performance, Gong et al. (2020) also highlighted that for GBDT methods there is no need of preprocessing the inputs data and the model is faster to train,

which is important when optimizing the parameters, because repeated training is needed.

In this context, this paper aims to develop a heat transfer coefficient predictive method for condensation of hydrocarbons applying artificial neural network and gradient boosted decision tree algorithms. The database considered in this analysis and described in Tab. 1 comprises 1245 experimental results, covering the hydrocarbons propane, propylene, isobutene and ethane, for tube diameters from 0.956 to 20.8 mm, mass velocities from 35 to 1000 kg/m²s and reduced pressures from 0.1 to 0.96.

Table 1. Experimental studies for condensation of hydrocarbons

Authors	**Hydrocarbons**	**Experimental conditions**			**d [mm]**	**Number of experimental results**
		G [kg/m2s]	**x [-]**	**Tsat [°C]**		
Conventional size						
Agra and Teke (2008)	R600a	47 - 118	-	30 - 43	4	35
Park et al. (2008)	R600a, R1270 and R290	100 - 300	0.1 - 0.9	40	8.8	75
Lee and Son (2010)	R290 and R600a	35.5 - 178.8	0 - 0.9	40	5.8 - 10.07	80
Macdonald and Garimella (2016a)	R290	150 - 450	0.1 - 0.9	30 - 94	7.75 - 14.45	278
Zhuang et al. (2016)	R170	100 - 250	0 - 1	-32 - 2	4	219
Longo et al. (2017)	R290 and R1270	75 - 400	0.12 - 0.95	30 - 40	4	133
Fries et al. (2019)	R290	150 - 400	0.07 - 0.89	34.5 - 46.8	14.65 - 20.8	39
Minichannels						
Del Col et al. (2014)	R290	100 - 1000	0 - 0.9	40	0.96	63
Liu et al. (2016)	R290	200 - 500	0.1 - 0.9	40 - 50	0.956 - 1.085	61
Lopez-Belchi et al. (2016)	R290	175 - 350	0.1 - 0.9	30 - 50	1.16	101
Del Col et al. (2017)	R1270	80 - 1000	0.1 - 0.9	40	0.96	113
Guo et al. (2018)	R290	200 - 400	0.1 - 0.9	35 - 45	2.00	187

2. MACHINE LEARNING METHODOLOGY

Table 2 displays the main dimensionless numbers for condensation flow. The number of input variables was estimated by applying the Buckingham's Pi Theorem, which resulted in four dimensionless numbers as input. For the selection of the input features, initially, the variance of each parameter was verified in a plot of the dimensionless numbers x HTC. A near-zero variance parameter provides few useful information and therefore should be eliminated. Then, a recursive feature elimination was applied, that consists of training the GBDT using all the dimensionless numbers and computing the importance of each feature in the HTC – which is an output of the method. Then, the least important features are removed, and the method applied again. During this process, the following criteria are obeyed: i) the final dimensionless numbers should have close values for the variable importance output; ii) the dimensionless numbers should be associated to different effects on the condensation process, for example, two Reynolds Numbers are not appropriate. The MAE and R² score of the method are analyzed in each iteration, avoiding an abrupt decrease of the model performance. The four dimensionless numbers resulting from this process were: Bd, Ga, Re_{lo}, and We_g.

The dataset of each experimental study was randomly divided into training and testing set, with the ratio of distribution varying between the models. This distribution was considered since the number of studies is reduced, and each of them presents unique experimental conditions.

Table 2. Dimensionless numbers usually applied in two-phase flows

$Re_{ko} = \frac{GD}{\mu_k}; Re_{lo} = \frac{G(1-x)D}{\mu_l}; Re_{go} = \frac{GxD}{\mu_g}$	$Ga = \frac{g(\rho_l - \rho_g)D^3}{\mu_l^2}$
$Fr_{lo} = \frac{G^2}{gD\rho_l^2}; Fr_l = \frac{G(1-x)^2}{gD\rho_l^2}$	$X_{tt} = (\frac{\mu_l}{\mu_g})^{0.1}(\frac{\rho_g}{\rho_l})^{0.5}(\frac{1-x}{x})^{0.9}$
$We_{lo} = \frac{G^2 D}{\rho_l \sigma}; We_g = \frac{\rho_g u_g^2 D}{\sigma}$	$\alpha = (1 + 1.021 Fr_m^{-0.092}(\frac{\mu_l}{\mu_g})^{-0.368}(\frac{\rho_g}{\rho_l})^{\frac{1}{3}}(\frac{1-x}{x})^{\frac{2}{3}})^{-1}$
$Su_{ko} = \frac{Re_{ko}}{We_{ko}}$	$\frac{u_g}{u_l} = (\frac{x}{1-x})(\frac{\rho_l}{\rho_g})(\frac{1-\alpha}{\alpha})$
$Bd = \frac{g(\rho_l - \rho_g)D^2}{\sigma}$	

2.1 Artificial Neural Net

The software package employed to implement the ML methodologies was the python open-source scikit-learn (Pedregosa et al., 2011). The multi-layer perceptron with backpropagation was the used ANN algorithm. The neural net can be separated into three groups of layers: input layer, hidden layer and output layer. The learning process happens in the hidden layers and the complexity of the model depends on the number of hidden layers and nodes in each layer. The neurons are connected by weights and the signal transmitted by a neuron is controlled by the activation functions. Some commonly used functions are the logistic sigmoid function ($f(x) = 1/(1+exp(-x))$), hyperbolic tangent function ($f(x) = tanh(x)$) and rectified linear unit function ($f(x) = max(0, x)$). Riedmiller (1994) explains that the backpropagation algorithm consists of updating the weights according to the partial error concerning each weight (E/w) and a defined learning rate (ϵ).

Scikit-learn provides the possibility of using different solvers for updating the network's weight iterative: 'L-BFGS (quasi-Newton method)', 'sgd' (stochastic gradient descent) and 'adam'. L-BFGS was developed by Nocedal (1980) and approximates the Broyden–Fletcher–Goldfarb–Shanno (BFGS) algorithm using limited computer memory, therefore it is usually used for small datasets. Adam is a more recent optimization algorithm and refers to the stochastic gradient descent proposed by Kingma and Ba (2014). For updating the learning rates, the authors considered the first and second moments of the error gradients (mean and variance, respectively), and these moments can be estimated as a function of the constants in scikit-learn, respectively. For sgd and adam, the learning rate is adaptive. Finally, the regularization parameter is important to prevent overfitting. A small value of this parameter implies in good predictions for the training dataset, but the model may perform poorly in the testing set. An ideal value results on a model that is able to learn the pattern between input and output and avoid the outliers. Table 3 presents the optimal parameters.

Table 3. Optimized parameters for the MLPB

Parameters	**Optimized Value**
Training/Testing set	$60\%/40\%$
Activator	rectified linear unit function
Solver	adam
Regularization Parameter	10
Initial Learning Rate	0.001
$\boldsymbol{\beta_1}$	0.98
$\boldsymbol{\beta_2}$	0.99

2.2 Gradient Boosted Decision Trees

Gradient Boosted Decision Trees combines several weak regression tree models, each one fitted to the residuals of the previous tree until reach the stopping criteria. The loss functions that can be tested are least squares regression (ls), least absolute deviation (lad), 'huber' – a combination of ls and lad –, and quantile regression. According to Friedman et al. (2009), the main regularization strategies for Gradient Boosting Decision Tree are shrinkage and stochastic gradient boosting. Shrinkage consists of scaling the contribution of each three by a learning rate between 0 and 1. Choosing a large learning rate for the model, it can pass through the minimum value for the loss function, while a small one would take too long to train and may also reach a local minimum. The stochastic gradient boosting is a great tool to avoid that effect, which consists of using a subsample of the training data for the next iteration in the next tree. The final two parameters optimized are the number of regression tree trained and the maximum depth of each regression tree. Table 4 presents the optimized parameters.

Table 4. Optimized parameters for the GBDT

Parameters	**Optimized Value**
Training/Testing set	$30\%/70\%$
Loss Function	Least square
Learning rate	0.1
Subsample	0.5
Number of regression tree	500
Maximum depth of each tree	6

3. RESULTS

Moreira et al. (2020) evaluated 19 predictive models available in the literature with the database for condensation of hydrocarbons and none of them provided reasonable predictions for both mini and conventional channels. Del Col et al. (2014) proposed a correction factor for applying the Cavallini et al. (2006) model in the condensation of hydrocarbons in minichannels and it provided the best predictions for small diameter and conventional channels. In the present study, the transition between mini and conventional channels is characterize by a hydraulic diameter of 3 mm.

Table 5 presents a comparison among the predictions provided by the machine learning methods and the experimental database of each author. The GBDT method predicted 86.5% of the data within an error band of ±10%, and a MAE of 4.7% using only 30% of the data as training set. The MLPB method also provided satisfactory predictions, with a MAE of 8.5% and 91.2% of the predictions within an error band of ±20%. As seen in this table, the ML methods provide better predictions for all the experimental databases compared to the model of Cavallini et al. (2006). It is a fact that despite providing overall satisfactory predictions, the methods also have to capture the experimental behaviors when varying the operational parameters. Therefore, the capability of the ML methods to capture the heat transfer behaviors is analyzed in the following items.

Table 5. Statistical parameters resulting from the comparison of the experimental databases and machine learning methods $(MAE/\gamma_{10};\gamma_{20};\gamma_{30})$

	MLPB	**GBDT**	**Cavallini et al. (2006)**
Del Col et al. (2014/2017)	6.2/ 85.8; 97.2; 98.9	4.0/ 88.7; 99.4; 100	7.8/ 71.0; 91.5; 98.3
Guo et al. (2018)	11.1/ 60.4; 83.3; 91.7	8.5/ 62.5; 85.4; 100	21.5/ 12.5; 41.7; 85.4
Liu et al. (2016)	12.5/ 49.2; 82.0; 91.8	4.2/ 88.5; 96.7; 100	17.0/ 41.1; 60.7; 80.3
Lopez Belchi et al. (2016)	10.8/ 49.5; 89.2; 100	2.6/ 97.0; 100; 100	13.3/ 41.6; 77.2; 97.0
Park et al. (2008)	5.5/ 86.7; 98.7; 100	5.1/ 81.3; 97.3; 100	10.7/ 50.7; 88.0; 97.3
Agra and Teke (2008)	10.5/ 42.9; 91.4; 100	4.6/ 88.6; 97.1; 100	16.3/ 28.6; 54.3; 97.1
Zhuang et al. (2016)	8.9/ 62.5; 95.0; 98.6	4.4/ 90.4; 96.8; 99.1	20.6/ 33.3; 50.7; 69.4
Longo et al. (2017)	14.1/ 39.1; 70.7; 91.0	4.9/ 84.2; 98.5; 100	38.4/ 12.0; 19.5; 33.8
Fries et al. (2018)	5.8/ 84.6; 97.5; 97.5	6.8/ 74.4; 92.3; 97.4	8.6/ 69.2; 97.4; 100
Lee and Son (2010)	12.9/ 60.0; 81.3; 87.5	5.9/ 80.0; 98.8; 100	17.8/ 31.3; 56.3; 83.8
MacDonald and Garimella (2016)	4.6/ 91.0; 98.6; 100	4.5/ 87.8; 99.3; 99.6	38.0/ 32.4; 51.4; 65.8
All mini	**9.0/ 67.4; 90.9; 97.2**	**4.3/ 87.6; 97.4; 100**	**12.4/ 51.3; 76.7; 93.5**
All convention	**8.3/ 70.2; 91.4; 96.7**	**4.8/ 86.0; 97.9; 99.5**	**19.7/ 29.8; 53.8; 80.3**
All dataset	**8.5/ 69.3; 91.2; 96.9**	**4.7/ 86.5; 97.8; 99.7**	**17.5/ 36.5; 60.9; 84.4**

3.1 Effect of mass velocity and vapor quality

Figure 1 displays the effects of mass velocity and vapor quality on the heat transfer behavior for conventional and minichannels, according to the experimental data of Del Col et al. (2014) and Macdonald and Garimella (2016) and the proposed methods. According to this figure, the methods capture the increase in the HTC with the increase of mass velocity and vapor quality. The larger deviations for the MLPB method consist of Lee and Son (2010) data, more specifically at vapor qualities near to zero and reduced mass velocities. For mass velocity of 50 kg/m²s and the range of diameter evaluated by Lee and Son (2010), the heat transfer coefficient is dominated by gravitational effects, which can be modeled with the help of the Nusselt theory for laminar falling film. Indeed, using the flow pattern map proposed by Thome et al. (2003) for conventional channels, Lee and Son (2010) data are classified as stratified/stratified wavy. In that case, HTC is only marginally affected by de vapor quality. Such behavior is captured reasonably well by the MLPB. A comparison of the mean experimental and predicted HTC values for Lee and Son (2010) data reveals a maximum deviation of 4% and therefore, those outliers data are not representative and may be associated to experimental inaccuracies. The GBDT method over-predicted only three data points, consisting two of them of data of Zhuang et al. (2016) for saturation temperature of -4 °C, mass velocity of 255 kg/m²s and vapor quality lower than 0.1. The other data point consists of Macdonald and Garimella (2016) results for a mass velocity of 150 kg/m²s, channel diameter of 7.75 mm, saturation temperature of 94°C and vapor quality of 0.2.

3.2 Effect of saturation temperature

The methods also capture the effect of saturation temperature on the HTC for conventional and minichannels, as revealed in Fig. 2.

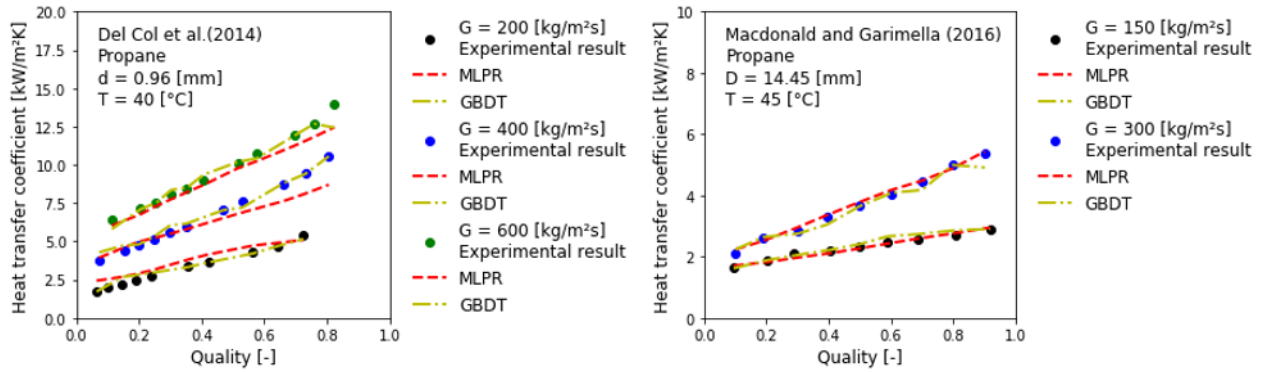

Figure 1. Effect of mass velocity and vapor quality on the HTC according to the prediction methods and the data of Del Col et al. (2014) and Macdonald and Garimella (2016)

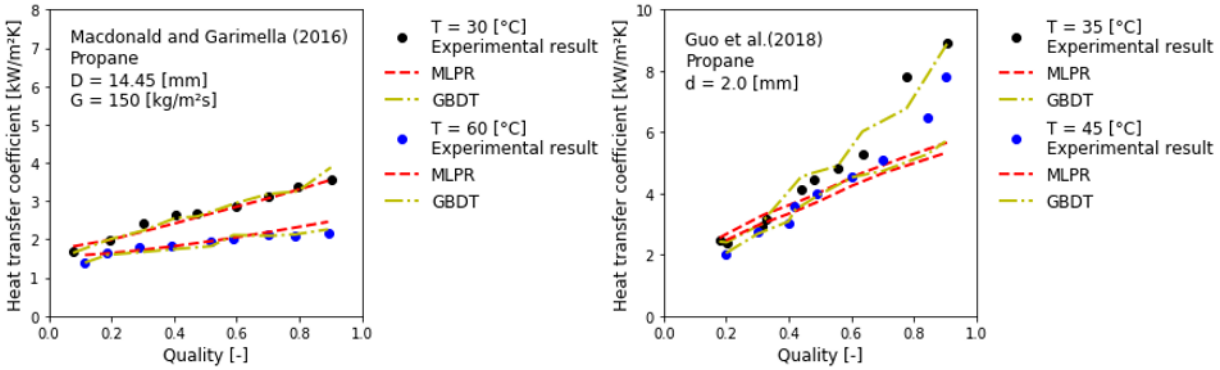

Figure 2. Effect of saturation temperature on the HTC according to the prediction methods and the data of Guo et al. (2018) and Macdonald and Garimella (2016)

However, MLPB underestimated Guo et al. (2018) data for high vapor qualities. This result was expected due to the incompatibilities of Del Col et al. (2014) and Guo et al. (2018) data. For the experimental condition of propane at mass velocity of 200 kg/m²s, Guo et al. (2018) and Del Col et al. (2014) presented similar results. However, Guo et al. (2018) performed their experiments in a tube of higher diameter than Del Col et al. (2014) did and it should have presented lower value of HTC. In fact, the data of Guo et al. (2018) display peculiar heat transfer behaviors. The GBDT method predicts a sudden increase in the HTC for high vapor quality and a saturation temperature of 35°C. This behavior agrees with the data of Guo et al. (2018) for , however, it is important to highlight that a similar behavior was not observed by any other author and may be due to the experimental uncertainties and the possible adoption of inappropriate measurement procedures.

3.3 Effect of channel diameter

The response of the methods to the effect of the channel diameter is evaluated through a comparison of their predictions and the databases of Lee and Son (2010) and MacDonald and Garimella (2016) in Fig. 3. Both MLPB and GBDT methods are reasonably accurate comparing to the experimental data. There is not a clear dependence of the performances of the ML methods with the channel diameter and the larger deviations seem to be more dependent on the saturation temperature, vapor quality and mass velocity.

3.4 Effect of channel shape

The methods do not capture explicitly the effect of channel geometry since this variable was not considered as an input parameter. As reported by Liu et al. (2016), the square channels tend to present higher HTC than circular channels. However, in general, the ML methods do not underestimate the HTC results obtained by Liu et al. (2016) and Lopez-Belchi et al. (2016), providing reasonable predictions for both geometries. In this analysis, the use of the equivalent and hydraulic diameter were evaluated. The difference between the diameters consists in considering the heat transfer perimeter of the channel for equivalent diameter and the wet perimeter for hydraulic diameter. Thus, if the channel is cooled in the entire perimeter, they present similar values. In the hydrocarbon database, differences in the equivalent and hydraulic diameter are observed only for the database of Lopez-Belchi et al. (2016) and the use of the equivalent diameter provided poor predictions of their data, while the use of hydraulic diameter has provided satisfactory predictions.

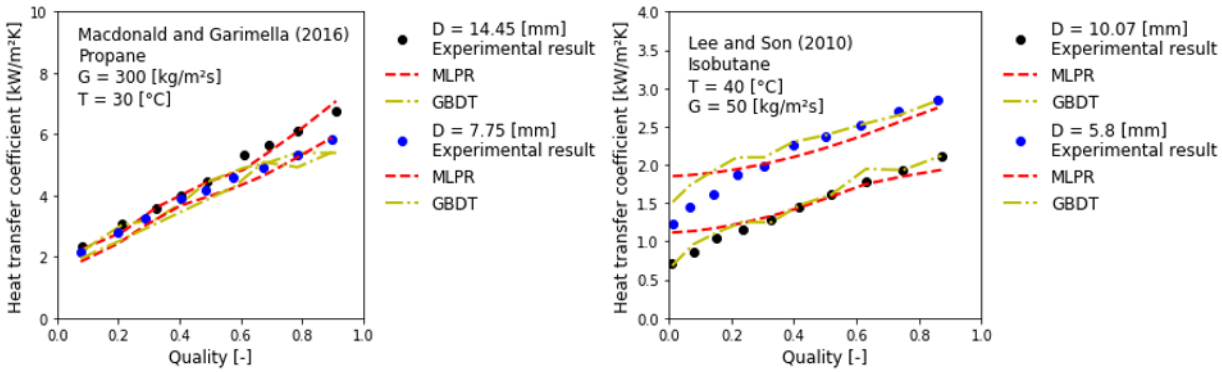

Figure 3. Effect of channel diameter on the HTC according to the prediction methods and the data of Macdonald and Garimella (2016) and Lee and Son (2010)

3.5 Effect of reduced pressure

The vapor specific volume, viscosity, liquid thermal conductivity and vaporization enthalpy are linked to the heat transfer coefficient and they vary drastically with reduced pressure. The vaporization enthalpy decreases as reduced pressure increases. Therefore, under similar mass velocity and heat flux conditions, a large amount of vapor is condensed at higher fluid temperatures, which provides an increase of the liquid film thickness and, consequently, a reduction in the HTC. A decrease of the vapor specific volume ratio causes a reduction of the drift velocity and, consequently, of the interfacial shear stress, increasing the liquid film thickness. The reduction in the liquid thermal conductivity provides an increase in the thermal resistance associated with the conduction through the liquid film and, consequently, reduces the HTC. Despite the disparity of the properties, the methods provided reasonable predictions over all the range of reduced pressure, from 0.1276 to 0.9529.

3.6 Flow Pattern

The dominant effects during condensation in small diameter channels are associated to inertial and surface tension forces, which can be characterized by the Weber number. Considering the flow pattern prediction method proposed by Nema, Fronk and Garimella (2014), inertial effects are dominant for mist flow and annular flow, while the predominance of surface tension is more evident for We_g, when bubble flow occurs. Figure 4 presents the deviation of the predictions relative to the experimental data with Weber Number for the MLPB and GBDT methods. For mist flow, the large difference in velocities between the vapor core and the liquid film induces the liquid entrainment, which implies on the reduction of the liquid film thickness. The HTC under this flow pattern is fully dominated by convective effects and therefore proportional to the liquid film thickness. For the MLPB, the lowest deviations occur for convective dominated condensation (mist and annular flow) and there is an increase in the MAE when surface tension forces become dominant (bubble flow). Based on Fig. 4, it can be concluded that the GBDT performed well for all the flow patterns.

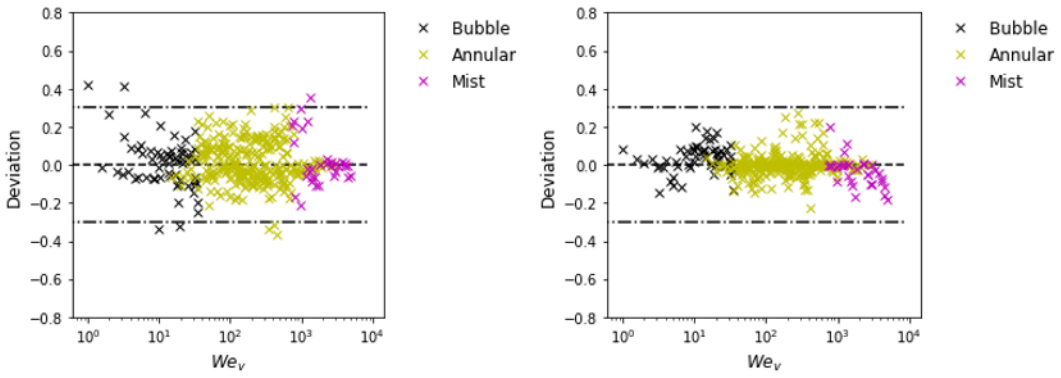

Figure 4. Variation with the Weber number of the deviations relative to the experimental data segregated according to flow pattern for the MLPB and GBDT method

Inertial and gravitational forces are dominant for conventional channels and their respective degree of predominance on the heat transfer process can be characterized through the Froude number. Figure 5 illustrates the deviation of the ML methods relative to the experimental data segregating according to the flow patterns based on Nema, Fronk and Garimella (2014). The convective effects are dominant in mist, annular and disperse wave flow patterns. Disperse wave

flow occurs for higher mass velocities when compared to stratified wavy flow and can be characterized by the occurrence of many secondary waves. For the MLPB, the largest deviations occur for Froude numbers lower than 0.1, consisting of bubble flow pattern and gravitational dominant condensation, specifically Lee and Son (2010) and Zhuang et al. (2016) data. Table 6 presents a comparison of the MLPB and GBDT predictions with the experimental database with the data segregated according to the flow pattern. As observed, the ML methods provide reasonable predictions independent of the flow patterns, with the large MAE occurring for bubble flow in conventional channels. Despite being flow pattern based, the mechanistic model provided worst results than the ML methods independent of the flow pattern. Therefore, it can be concluded that the models can perform well for all the condensation process, including convective, surface tension and gravitational dominant condensation.

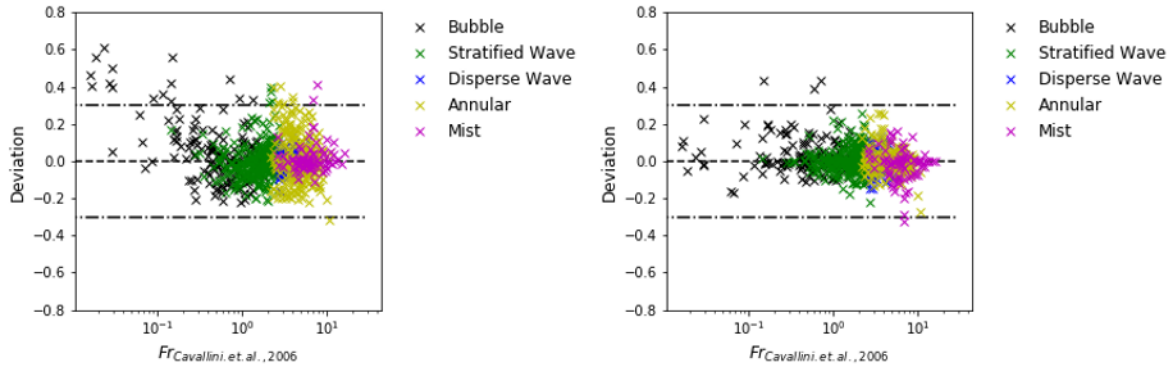

Figure 5. Variation with the Froude number of the deviations relative to the experimental data segregated according to flow pattern for the MLPB and GBDT method

Table 6. MAE of the ML methods and Cavallini et al. (2006) model for the data segregated according to the flow pattern (Nema, Fronk and Garimella, 2014)

		MAE (MLPB)	**MAE (GBDT)**	**MAE (Cavallini et al., 2006)**
Minichannels	Mist	9.0	6.1	10.1
	Annular	8.6	3.6	11.4
	Bubble	10.4	5.9	16.7
Conventional channels	Mist	4.6	6.0	18.3
	Annular	10.2	4.0	17.4
	Disperse Wave	4.0	4.3	18.0
	Stratified Wave	6.7	4.6	23.2
	Bubble	12.9	6.5	19.0

3.7 Processing Time

The machine learning methods present also superior performance than the mechanistic models concerning processing time. This additional positive aspect of the ML methods was proved based on a simulation of a tube in tube condenser considering 100 discrete elements and for an internal tube diameter of 0.96 mm, mass velocity of 400 kg/m²s and assuming full condensation process of propane, as illustrated in Fig. 6. In this analysis, the MLPB and GBDT methods and Cavallini et al. (2006) model were compared. The simulation using the Cavallini et al. (2006) model presented a processing time 900% higher than MLPB, which presented a 15% lower processing time than GBDT.

3.8 Comparison between MLPB and GBDT

Despite providing worse overall prediction than GBDT, the neural net method presents some advantages. The MLPB displays smoother variations in the HTC when varying x, as illustrated in Fig. 7, without any abrupt changes as observed for the GBDT. This behavior indicates that GBDT is more dependent on the training data and, therefore, the neural net may capture better the trends observed in the HTC experimentally, and, when applied to independent data, should provide better predictions. The generality of the methods were evaluated by comparing them against non-hydrocarbon databases. In this analysis the minichannel data of Del Col et al. (2010) for HFO R1234yf and Del Col et al. (2015) for HFO R1234ze(E) were considered.

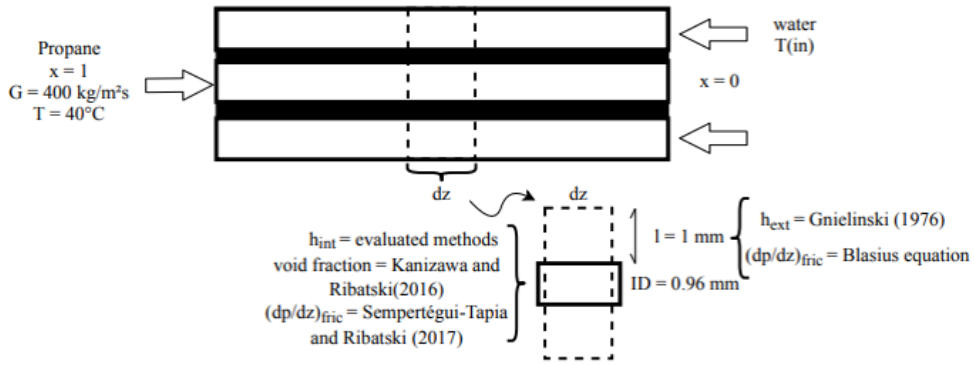

Figure 6. Schematics of a discretized tube in a tube heat exchanger

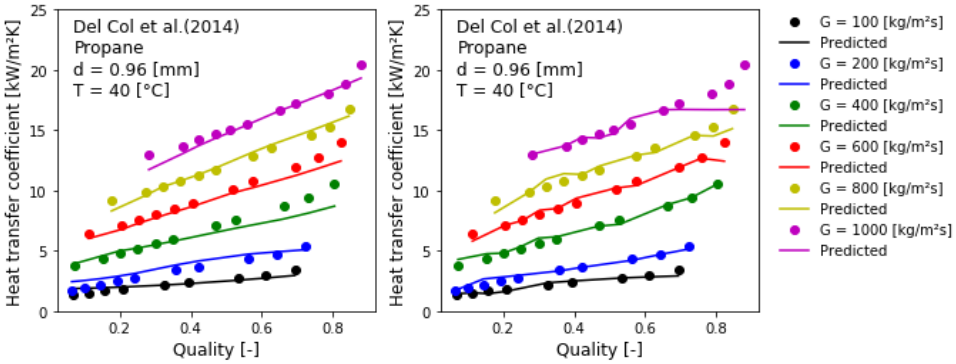

Figure 7. Comparison between the predictions of MLPB and GBDT for Del Col et al. (2014) data

As seen in Fig. 8, the MLPB method provided better overall predictions. Concerning conventional channels, Fig. 9 displays the comparison of the predictions of ML methods and the experimental results for the fluids R32, R22 and R134a from Cavallini et al. (2001). As for minichannels, the MLPB method provided better overall predictions, corroborating the above hypothesis. These results suggest the applicability of the MLPB method for other fluids, even without using them for training the model, which demonstrates the power of this tool to be applied to the design of heat exchangers. In this context, it is suggested further tests to be performed for other fluids. However, despite that, it seems that the MLPB is a promising method for developing a universal heat transfer prediction procedure. The GBDT method is more sensitive to the training set and therefore should be carefully used for other conditions. However, the GBDT presented satisfactory predictions using only 30% of the data for training and should be also considered as a reasonable approach for developing a universal HTC model.

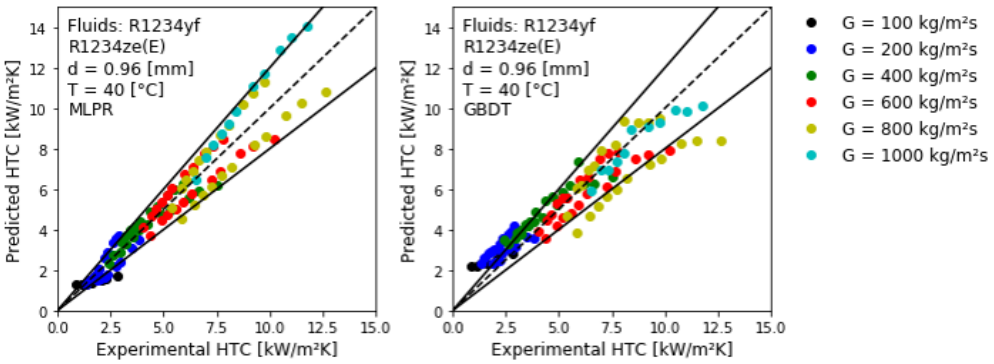

Figure 8. Comparison of MLPB and GBDT predictions and experimental results for R1234y and R1234ze(E)

4. CONCLUSIONS

In the present study, the multi-layer perceptron with backpropagation and gradient boosted decision tree were successfully optimized, trained, and validated using 1245 experimental data from the literature. The dimensionless numbers used as input parameters for the machine learning methods that provided the best performance were: Bd, Ga, Re_{lo}, and We_v.They are able of capturing the main hydrodynamic and heat transfer effects such as inertia, viscosity, gravity and surface tension forces.

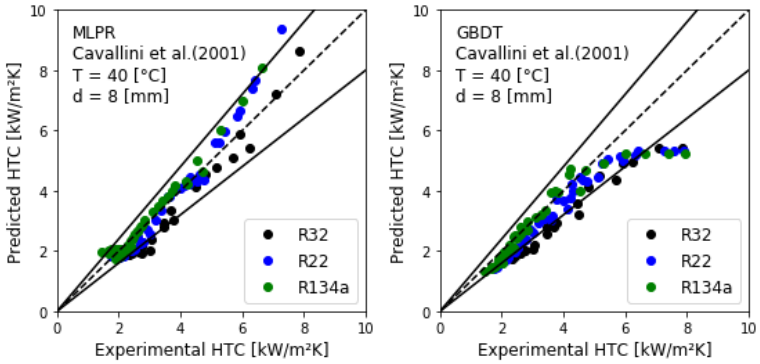

Figure 9. Comparison of MLPB and GBDT predictions and experimental results for R32, R22 and R134a

The MLPB and GBDT methods provided satisfactory predictions independent of the database and they were also able to predict the effects on the HTC of the vapor quality, mass velocity, saturation temperature, channel diameter and flow pattern when compared to the experimental results. The ML methods provided better predictions than Cavallini et al. (2006) model independent of the database. Besides, they presented 90% lower processing time than the model of Cavallini et al. (2006) in a simulation of a tube-in-tube condenser. Finally, the MLPB and GBDT method also provided reasonable predictions for the condensation of the HFOs R1234yf and R1234ze(E) in minichannels and for the fluids R32, R22 and R134a in conventional channels. Therefore, it is concluded that the ML methods represent a valuable tool for predicting the heat transfer coefficient during condensation of hydrocarbon and should be considered for developing a universal HTC model.

5. ACKNOWLEDGEMENTS

This study was financed in part by the Coordenação de Aperfeiçoamento de Pessoal de Nível Superior – Brasil (CAPES) – Finance Code 001. The authors acknowledge the support through a Thematic Grant provided by FAPESP (São Paulo Research Foundation, Brazil) under Contract Number 2016/09509-01. The authors gratefully acknowledge the scholarship to the second author provided by CNPq (National Council of Scientific and Technological Development, Brazil) under Contract Number 132528/2017-7.

6. REFERENCES

Ağra, Ö.; Teke, İ. Experimental investigation of condensation of hydrocarbon refrigerants (R600a) in a horizontal smooth tube. *International communications in heat and mass transfer*, v. 35, n. 9, p. 1165-1171, 2008.

Ahmad, M. W.; Reynolds, J.; Rezgui, Y. Predictive modelling for solar thermal energy systems: A comparison of support vector regression, random forest, extra trees and regression trees. *Journal of Cleaner Production*, v. 203, p. 810-821, 2018.

Balcilar, M.; Dalkilic, A. S.; Wongwises, S. Artificial neural network techniques for the determination of condensation heat transfer characteristics during downward annular flow of R134a inside a vertical smooth tube. *International Communications in Heat and Mass Transfer*, v. 38, n. 1, p. 75-84, 2011.

Cavallini, A., et al. Experimental investigation on condensation heat transfer and pressure drop of new HFC refrigerants (R134a, R125, R32, R410A, R236ea) in a horizontal smooth tube. *International Journal of Refrigeration* 24.1 (2001): 73-87.

Cavallini, A., et al. Condensation in horizontal smooth tubes: a new heat transfer model for heat exchanger design. *Heat transfer engineering*, v. 27, n. 8, p. 31-38, 2006.

Del Col, D., Torresin, D., Cavallini, A. Heat transfer and pressure drop during condensation of the low GWP refrigerant R1234yf. *International Journal of refrigeration* 33.7 (2010): 1307-1318.

Del Col, D., et al. Experimental results and design procedures for minichannel condensers and evaporators using propylene. *International Journal of Refrigeration*, v. 83, p. 23-38, 2017.

Del Col, D., et al. Condensation heat transfer and two-phase frictional pressure drop in a single minichannel with R1234ze (E) and other refrigerants. *International Journal of Refrigeration* 50 (2015): 87-103.

Del Col, D.; Bortolato, M.; Bortolin, S. Comprehensive experimental investigation of two-phase heat transfer and pressure drop with propane in a minichannel. *International Journal of Refrigeration*, v. 47, p. 66-84, 2014.

Demir, H.; Ağra, Ö.; Atayilmaz, Ş.Ö. Generalized neural network model of alternative refrigerant (R600a) inside a smooth tube. *International Communications in Heat and Mass Transfer*, v. 36, n. 7, p. 744-749, 2009.

Fries, S.; Skusa, S., Luke, A. Heat transfer and pressure drop of condensation of hydrocarbons in tubes. *Heat and Mass Transfer* 55.1 (2019): 33-40.

Gong, M., et al. Gradient boosting machine for predicting return temperature of district heating system: A case study for residential buildings in Tianjin. *Journal of Building Engineering*, v. 27, p. 100950, 2020.

Guo, Q.; Li, M.; Gu, H. "Condensation heat transfer characteristics of low-GWP refrigerants in a smooth horizontal mini tube." *International Journal of Heat and Mass Transfer* 126 (2018): 26-38.

Hastie, T.; Tibshirani, R.; Friedman, J. Boosting and additive trees. In: *The elements of statistical learning*. Springer, New York, NY, 2009. p. 337-387.

Kanizawa, F.T.; Ribatski, G. Void fraction predictive method based on the minimum kinetic energy. *Journal of the Brazilian Society of Mechanical Sciences and Engineering*, v. 38, n. 1, p. 209-225, 2016.

Kingma, D.P.; BA, J. Adam: A method for stochastic optimization. arXiv preprint arXiv:1412.6980, 2014. Lee, H.S.; Son, C.H. Condensation heat transfer and pressure drop characteristics of R-290, R-600a, R-134a and R-22 in horizontal tubes. *Heat and mass transfer*, v. 46, n. 5, p. 571-584, 2010.

Liu, N.; Xiao, H.; LI, J. Experimental investigation of condensation heat transfer and pressure drop of propane, R1234ze (E) and R22 in minichannels.*Applied Thermal Engineering*, v. 102, p. 63-72, 2016.

Longo, G.A., et al. Saturated vapour condensation of HFC404A inside a 4 mm ID horizontal smooth tube: Comparison with the long-term low GWP substitutes HC290 (Propane) and HC1270 (Propylene). *International Journal of Heat and Mass Transfer*, v. 108, p. 2088-2099, 2017.

López-Belchí, A., et al. GMDH ANN to optimise model development: Prediction of the pressure drop and the heat transfer coefficient during condensation within mini-channels. *Applied Thermal Engineering*, v. 144, p. 321-330, 2018.

López-Belchí, A., et al. Condensing two-phase pressure drop and heat transfer coefficient of propane in a horizontal multiport mini-channel tube: Experimental measurements. *International Journal of Refrigeratio*n 68 (2016): 59-75.

Macdonald, M.; GARIMELLA, S. Hydrocarbon condensation in horizontal smooth tubes: Part II–Heat transfer coefficient and pressure drop modeling. *International Journal of Heat and Mass Transfer*, v. 93, p. 1248-1261, 2016.

Mohanraj, M.; Jayaraj, S.; Muraleedharan, C. "Applications of artificial neural networks for thermal analysis of heat exchangers–a review." *International Journal of Thermal Sciences* 90 (2015): 150-172.

Moreira, T.A., et al (submitted). Flow boiling and convective condensation of hydrocarbons: A state-of-the-art literature review. *Applied Thermal Engineering*, 2020.

Nema, G.; Garimella, S.; Fronk, B. M. Flow regime transitions during condensation in microchannels. *International journal of refrigeration*, v. 40, pp. 227-240, 2014.

Nocedal, J. Updating quasi-Newton matrices with limited storage. *Mathematics of computation*, v. 35, n. 151, p. 773-782, 1980.

Park, K.J.; Jung, D.; Seo, T. Flow condensation heat transfer characteristics of hydrocarbon refrigerants and dimethyl ether inside a horizontal plain tube. *International journal of multiphase flow*, v. 34, n. 7, p. 628-635, 2008.

Pedregosa, F., et al. Scikit-learn: Machine learning in Python. *The Journal of machine Learning research*, v. 12, p. 2825-2830, 2011.

Qian, N., et al. Predicting heat transfer of oscillating heat pipes for machining processes based on extreme gradient boosting algorithm. *Applied Thermal Engineering*, v. 164, p. 114521, 2020.

Riedmiller, M. Advanced supervised learning in multi-layer perceptrons—from backpropagation to adaptive learning algorithms. *Computer Standards* & Interfaces, v. 16, n. 3, p. 265-278, 1994.

Touzani, S.; Granderson, J.; Fernandes, S. Gradient boosting machine for modeling the energy consumption of commercial buildings. *Energy and Buildings*, v. 158, p. 1533-1543, 2018.

Zhuang, X. R. et al. Experimental investigation on flow condensation heat transfer and pressure drop of R170 in a horizontal tube. *International Journal of Refrigeration*, v. 66, p. 105-120, 2016.

7. RESPONSIBILITY NOTICE

The authors are the only responsible for the printed material included in this paper.